

In Vivo Loss of Function Screening Reveals Carbonic Anhydrase IX as a Key Modulator of Tumor Initiating Potential in Primary Pancreatic Tumors^{1,2}

Nabendu Pore^{*,3}, Sanjoo Jalla^{*,3}, Zheng Liu^{*}, Brandon Higgs^{*}, Claudio Sorio[†], Aldo Scarpa[†], Robert Hollingsworth^{*}, David A. Tice^{*} and Emil Michelotti^{*}

^{*}MedImmune, LLC, Gaithersburg, MD, USA; [†]ARC-NET Research Centre and Department of Pathology and Diagnostics, University of Verona Medical School, Verona, Italy

Abstract

Reprogramming of energy metabolism is one of the emerging hallmarks of cancer. Up-regulation of energy metabolism pathways fuels cell growth and division, a key characteristic of neoplastic disease, and can lead to dependency on specific metabolic pathways. Thus, targeting energy metabolism pathways might offer the opportunity for novel therapeutics. Here, we describe the application of a novel *in vivo* screening approach for the identification of genes involved in cancer metabolism using a patient-derived pancreatic xenograft model. Lentiviruses expressing short hairpin RNAs (shRNAs) targeting 12 different cell surface protein transporters were separately transduced into the primary pancreatic tumor cells. Transduced cells were pooled and implanted into mice. Tumors were harvested at different times, and the frequency of each shRNA was determined as a measure of which ones prevented tumor growth. Several targets including carbonic anhydrase IX (CAIX), monocarboxylate transporter 4, and anionic amino acid transporter light chain, xc- system (xCT) were identified in these studies and shown to be required for tumor initiation and growth. Interestingly, CAIX was overexpressed in the tumor initiating cell population. CAIX expression alone correlated with a highly tumorigenic subpopulation of cells. Furthermore, CAIX expression was essential for tumor initiation because shRNA knockdown eliminated the ability of cells to grow *in vivo*. To the best of our knowledge, this is the first parallel *in vivo* assessment of multiple novel oncology target genes using a patient-derived pancreatic tumor model.

Neoplasia (2015) 17, 473–480

Introduction

Altered energy metabolism is a hallmark of cancer [1]. Important metabolic genes have been found to be the direct targets of oncogenes resulting in addiction to specific metabolic pathways [2]. For example, while normal cells support energy production following glucose deprivation by shifting to fatty acid oxidation, tumor cells expressing constitutively activated AKT are addicted to glucose consumption and are not viable under glucose-restricted conditions [3]. In addition to glucose consumption, recent literature indicates an increased reliance of tumor cells on specific amino transporters as well as pathways dedicated to maintenance of pH homeostasis. Within these three areas of interest, we have identified 12 genes implicated in providing tumors with the necessary metabolic adaptations to allow the establishment of anabolic processes and consequent tumor proliferation.

Our goal was to develop methods enabling a direct head-to-head comparison of the requirement for these genes in tumor development.

Such studies would be best carried out *in vivo* due to the likely alterations of tumor metabolism imparted by microenvironment factors such as hypoxia and competition/symbioses with the stromal

Address all correspondence to: Nabendu Pore, PhD or Emil Michelotti, PhD, One MedImmune Way, Gaithersburg, MD 20878.

E-mail: poren@medimmune.com

¹ C.S. and A.S. were supported by the European Community Project CAM-PaC (grant agreement no. 602783), AIRC grant no.12182 and the FIMP, Italian Ministry of Health (CUP_J33G13000210001).

² This article refers to supplementary materials, which are designated by Supplementary Table 1 and Supplementary Figures 1 and 2 and are available online at www.neoplasia.com.

³ Both authors contributed equally to this work.

Received 13 February 2015; Revised 2 May 2015; Accepted 5 May 2015

© 2015 The Authors. Published by Elsevier Inc. on behalf of Neoplasia Press, Inc. This is an open access article under the CC BY-NC-ND license (<http://creativecommons.org/licenses/by-nc-nd/4.0/>).

1476-5586

<http://dx.doi.org/10.1016/j.neo.2015.05.001>

compartment. As one possible approach, efforts have been made to develop transgenic mice and knockout mice containing germline mutations in candidate oncogenes [4]. Generating these genetically engineered mouse models is, however, time consuming and often does not reflect human disease.

To accelerate the systematic analysis of cancer genes *in vivo*, scientists have adapted loss of function screening by downregulating important genes using the short hairpin RNA (shRNA) technology [5–8]. These screens can be run in a pooled format in which numerous shRNAs can be queried in parallel. The use of an established cell line in such studies to validate the requirement for metabolic genes may yield misleading results due to metabolic alterations introduced by adaptations to prolonged growth in culture [9]. To avoid these and other potential artifacts, patient-derived xenografts (PDXs) are increasingly being used for *in vivo* studies [10]. We therefore used a pooled shRNA library consisting of 12 metabolism targets to assess the requirement for each of these genes in the growth of a pancreatic PDX model (herein referred to as PDX15) [11]. Of the 12 novel cell-surface metabolism targets, three [carbonic anhydrase IX (CAIX), monocarboxylate transporter 4 (MCT4), and anionic amino acid transporter light chain, xc- system (xCT)] were chosen to further validate the results of the shRNA screen. Furthermore, we show that one of these targets, CAIX, is enriched in tumor initiating cells (TICs) and required to initiate tumors *in vivo*. To our knowledge, this is the first pooled shRNA screen using a PDX model.

Materials and Methods

Preparation of Single-Cell Suspensions of Tumor Cells

Tumors excised from animals were minced using sterile scalpel blades. To obtain single-cell suspensions, the tumor pieces were mixed with 200 units of ultrapure collagenase III (Worthington Biochemicals, Freehold, NJ) per milliliter of Hank's balanced salt solution (HBSS). The tumor suspension was incubated at 37°C for approximately 1 hour, with mechanical disruption every 15 to 20 minutes by pipetting with a 5-ml pipette. At the end of the incubation, cells were filtered through a 70- μ m nylon mesh and washed twice with HBSS.

Enrichment of Epithelial Cells

Epithelial cells from single-cell suspensions were obtained by using an EasySep Human EpCAM Positive Selection Kit. Cells in the single-cell suspension were targeted with Tetrameric Antibody Complexes recognizing EpCAM and dextran-coated magnetic particles. Labeled cells were separated using an EasySep magnet. Enriched cells were washed once, and the cell number was counted on a Vi-cell.

Pooled shRNA Screening

pLKO.1 lentiviral particles encoding shRNAs against the different targets were obtained from Sigma-Aldrich Corp (St Louis, MO), and a library was assembled in the following way: The efficiency of knockdown of different shRNAs for the respective targets (five shRNAs per target) was evaluated, and the top two shRNAs were chosen for library construction (representative data in Supplementary Figure 1). Thus, we assembled a library of shRNAs composed of 27 shRNA hairpins [24 shRNAs for 12 different targets, Aurora B shRNA (positive control), Non Targeting (NT)-shRNA (negative control), and Green fluorescent protein (GFP)-shRNA (negative control)]. Thereafter, EpCAM+ primary epithelial tumor cells were isolated

from PDX15 tumors and separately transduced with the 27 different shRNAs in tissue culture flasks (Multiplicity of infection (MOI) \sim 1). Forty-eight hours post-transduction, cells individually transduced with respective shRNAs were harvested and combined into a single pool (starting pool). Thereafter, 3×10^6 cells of the starting pool ($\sim 1 \times 10^5$ cells/shRNA) were implanted into Recombination Activating Gene 2 (RAG2) KO mice. The frequency of each shRNA in the starting pool is described in Supplementary Table 1. After 3 to 4 weeks, mice were sacrificed, and tumors were harvested. Genomic DNA was isolated from the starting pool and tumors by using the QIAamp DNA Mini Kit. To amplify the shRNAs integrated into genomic DNA, polymerase chain reaction (PCR) was performed for 30 cycles by using Accu Prime Kit (Invitrogen, Waltham, MA), with 1 μ g of total chromosomal DNA and the primer pair described below. PCR products were purified and quantitated by Quant-iT DNA Assay Kit (Invitrogen). All samples, including the starting pool, were pooled at equal proportions and analyzed by quantitative sequencing (Illumina, San Diego, CA). Sequencing reads were deconvoluted using PERL software by segregating the sequencing data by barcode and matching the shRNA stem sequences to those expected to be present in the shRNA pool, allowing for mismatches of up to three nucleotides. The frequency of each shRNA was compared between the starting pool and each established tumor.

Primers for Amplifying shRNAs

The forward primer with Illumina adapter sequence is given as follows: ACAACTCTTTCCCTACACGACGCTCTTCCGATCTTTTCGATTTCTTGGC.

The reverse primer with Illumina adapter sequence is given as follows: CTCGGCATTCCCTGCTGAACCGCTCTTCCGATCTGATGAATACTGCCAT.

Statistical Analysis for shRNA Data Set

The data were \log_2 transformed before analysis. Independent samples *t* tests were performed on the \log_2 transformed data using Prism 6.03 where $P < 0.05$ was considered significant.

RNA Extraction and Quantitative PCR

Total RNA was isolated by using RNeasy Kit (Qiagen, Frederick, MD) according to the manufacturer's protocol. To detect the transcripts of interest, quantitative PCR (qPCR) was carried out using One-Step Quantitative RT-PCR System (Life Technologies, Grand Island, NY) with the respective TaqMan primer probes. Reactions were performed using an ABI Prism 7900 Sequence Detector (Life Technologies). All reactions were performed in triplicate. Results were normalized to the housekeeping gene (*18S*). Relative gene expression was calculated by using the $2^{-\Delta\Delta C_t}$ method.

Fluorescence-Activated Cell Sorting

Dissociated cells (0.5 to 1 million) were plated in 100 μ l of HBSS onto a round-bottom, tissue culture-treated 96-well plate (BD Falcon) and washed twice with HBSS containing 2% heat-inactivated FBS [fluorescence-activated cell sorting (FACS) buffer] and resuspended in cold FACS buffer. Antibodies were added and incubated for 20 minutes at 4°C. The sample was washed twice with cold FACS buffer and resuspended in cold FACS buffer containing 4',6-diamidino-2-phenylindole (1 μ g/ml final concentration). The antibodies used were anti-EpCAMPerCp-Cy5.5 purchased from eBioscience Inc

(San Diego, CA), anti-CD44-APC and anti-CD24-fluorescein isothiocyanate purchased from Life Technologies, anti-H2Kd-PE purchased from BD Biosciences San Jose, CA), and anti-CAIX-PE (R&D Systems, Minneapolis, MN). In all experiments using human xenograft tissue, live cells were gated through the use of 4',6-diamidino-2-phenylindole (Sigma-Aldrich Corp). Side scatter and forward scatter profiles were used to eliminate cell doublets, and infiltrating mouse cells were eliminated by gating on H2Kd (mouse histocompatibility class I) negative cells. TICs (EpCAM+CD44+CD24+) and non-TICs (EpCAM+CD44-CD24-) were gated on epithelial cells positive for EpCAM. Unstained samples were used to set gates, and fluorescence minus one controls were used as compensation controls. Sorting was done using FACSAria (BD Immunocytometry Systems, Franklin Lakes, NJ). Cells were reanalyzed after sorting for purity, which was typically >97%. To determine the percentage of TICs and non-TICs in the tumors, the samples were analyzed using BD LSRII flow cytometer (BD Biosciences), and the data were analyzed using FlowJo software (TreeStar Inc, Ashland, OR).

In Vivo Studies

Human PDX15 xenografts were maintained as a serially passaged xenograft model using female RAG2 KO mice (Taconic, Hudson, NY). For *in vivo* tumorigenicity assays, sorted cells [EpCAM+CAIX (high) or EpCAM+CAIX (low)] were washed with serum-free HBSS, counted, and resuspended in a 1:1 HBSS and Matrigel mixture. Cells (5000, 1000, 500, or 100) either EpCAM+CAIX (high) or EpCAM+CAIX (low) were subcutaneously injected into the right and left flanks, respectively, of the same mouse using a 23-gauge needle. Mice were monitored weekly for tumor formation. Tumors were harvested when they reached ~2000 mm³ in size.

All procedures were performed in accordance with institutional guidelines in an Association for Assessment and Accreditation of Laboratory Animal Care (AAALAC)-accredited facility and were approved by the MedImmune, LLC Institutional Animal Care and Use Committee.

Results

The 12 genes chosen to be included in the shRNA library encode proteins that cover three critical areas of tumor metabolism implicated in tumorigenesis. CAIX and CAXII, Sodium hydrogen exchanger 1 (NHE1), MCT1, MCT4, and CD147 all function in reversing the intracellular acidification that occurs following reduction of pyruvate to lactic acid during glycolysis [12–14]. Glut1 and sodium dependent glucose co-transporter (SGLT1) are both glucose transporters upregulated in tumors [13]. Finally, ASC amino-acid transporter 2 Sodium-Independent (ASCT2), Neutral Amino Acid Transporter (LAT1), xCT, and Zinc transporter (ZIP4) are transporters of nutrients required for tumor growth [13,15,16]. Two shRNAs for each target, which showed >70% silencing efficiency, were selected for assembling the custom library (see Supplementary Figure 1 for representative data sets supporting selection of LAT1 and Aurora B shRNAs). Overall, 24 different shRNAs covering the 12 queried genes and one positive (Aurora B) and two negative (non-targeting and GFP) shRNA controls were included in the custom library. The shRNAs of the lentiviral-based shRNA library were separately transduced into EpCAM-enriched (epithelial) primary pancreatic (PDX15) tumor cells, and 48 hours post-transduction cells were combined into a single pool. Cells (3×10^6) from the starting pool were injected into RAG2 KO immunocompromised mice (Figure 1A). Tumors were harvested at different times during tumor growth, and

genomic DNA from the tumors and starting pool was extracted. The representations of the respective shRNA hairpins in the starting pool and the tumors were determined by high-throughput sequencing (Illumina). The relative abundance of the individual shRNAs in the starting pool varied between 2% and 6% of the total population, presumably due to modest differences in the transduction efficiency of the individual lentiviral preparations (Supplementary Table 1). The frequency of each shRNA was compared in the starting pool *versus* each established tumor. Cells transduced with non-silencing shRNA (NT-shRNA) constituted the bulk of the cells of the tumor at the end of the study, while cells transduced with positive control Aurora B shRNA were almost undetectable (Figure 1B). The relative abundance of shRNAs targeting each of the 12 targets queried in the screen was consistent in the replicate tumors (10–12 tumors per shRNA; Figures 1B and Supplementary Figure 2). To validate the results from the pooled shRNA screen, we selected three nutrient transporters, CAIX, MCT4, and xCT, to confirm their role in tumor growth as implicated previously [12,17–21].

CAIX, MCT4, and xCT were validated by knockdown using individual shRNAs in a non-pooled format. PDX15 primary pancreatic tumor cells were transduced with two separate shRNAs for each target and implanted separately into RAG2 KO mice. After 3 to 4 weeks, palpable tumors were easily observed in mice implanted with untreated tumor cells as well as tumor cells transduced with empty vector lentivirus. In contrast, no tumors were observed in mice that received cells in which the expression of hits from the pooled screen was knocked down individually (Table 1).

We focused on CAIX to decipher its role in tumorigenesis because it is a druggable target, as several CAIX-targeting therapeutic agents are at different phases of preclinical and clinical development [22], and because it was the top hit of the pooled shRNA screen (~91% decrease in prevalence with respect to the starting pool). The decrease in prevalence of individual shRNAs in a pooled shRNA screen could be the result of inhibition of either tumor initiation or tumor growth/maintenance. Recent data implicating CAIX as a driver of breast cancer “stemness” suggest the former may be relevant [23]. The relative expression of CAIX in the TIC and bulk tumor cell populations of the pancreatic 479 PDX model was therefore queried.

In pancreatic cancer, various cell surface proteins have been evaluated as stem cell markers, including EpCAM, CD44, CD24 [24], CD133 [25], and c-Met [26,27]. In one of the earlier studies, Li et al. demonstrated that EpCAM+CD44+CD24+ cells could initiate tumors when as few as 100 cells were injected into immune-deficient mice [24]. We used these markers to isolate TIC and non-TIC populations by FACS. Flow cytometry analysis indicated high CAIX expression in TICs (EpCAM+/CD44+/CD24+; Figure 2, A and B). Increased expression of CAIX was further confirmed by qPCR analysis using total RNA isolated from CD44+/CD24+ and CD44-/CD24- populations (Figure 2C), which suggests differential genetic or epigenetic regulation of CAIX between TIC and non-TIC cells *in vivo*.

The increased expression of CAIX in the TICs prompted us to investigate the role of CAIX in pancreatic PDX15 model tumor initiation. EpCAM+/CAIX (high) and EpCAM+CAIX (low) cell populations were isolated using FACS (Figure 3B) and tested for their tumor initiating capabilities when implanted in varying numbers (5000, 1000, 500, and 100 cells) into RAG2 KO mice and grown for 3 months. Four to 6 weeks post-implantation, we saw at least a doubling in the tumor formation rate for CAIX (high) cells *versus* CAIX (low) cells at all levels of tumor cell inoculation (Figure 3A and Table 2). Furthermore,

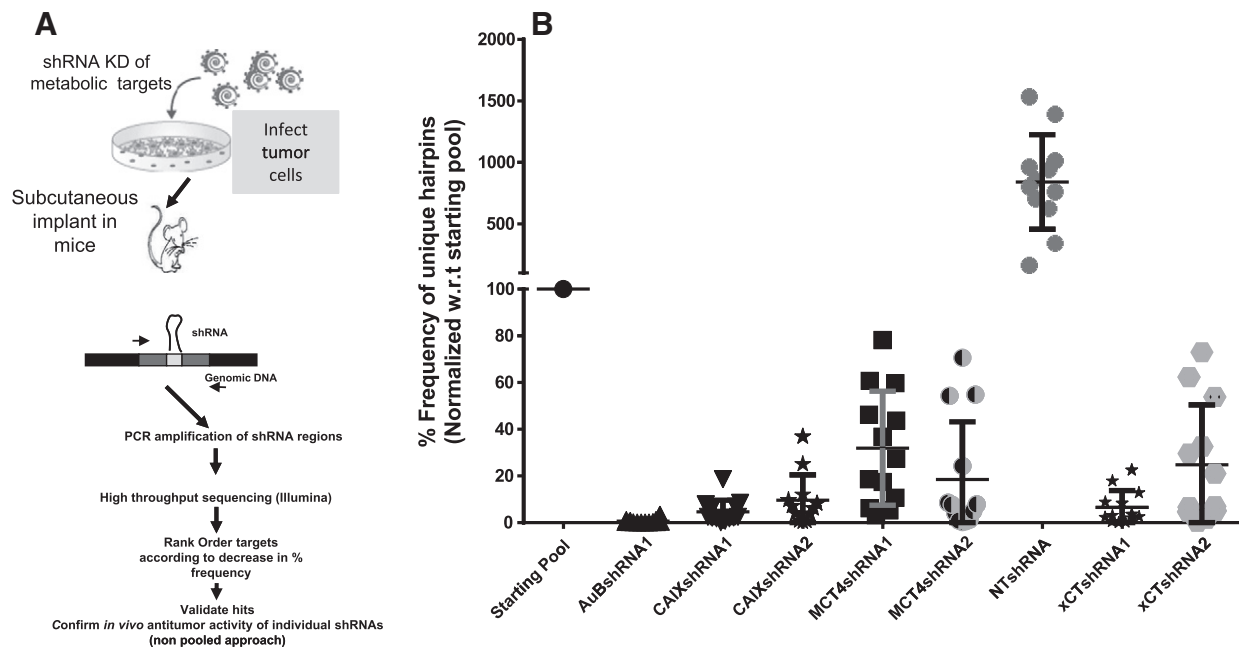


Figure 1. Schematic design of *in vivo* pooled shRNA screening strategy to identify novel targets for cancer metabolism. (A) Outline of the experimental design. (B) Percentage frequency of shRNA hairpins to selected targets present in tumors normalized with respect to the starting pool (injected cell population).

tumors that did initiate from CAIX (low) cells were four to eight times smaller than those initiated from CAIX (high) cells, indicating that CAIX may play a dual role in both tumor initiation and tumor proliferation.

To further examine if increased expression of CAIX has any functional significance in PDX15 tumor formation, we silenced CAIX expression in EpCAM⁺/CAIX (high) cells (5000 cells) with two specific shRNAs and implanted the cells into mice. CAIX silenced cells failed to initiate tumors, while tumors were observed in animals inoculated with the cells transduced with NT-shRNA (Figure 4A) or untransduced control (data not shown). Tumor growth rates of the treatment arms were followed for 60 days (summarized in Table 3). While a role in tumor proliferation cannot be ruled out, these results suggest that CAIX expression is required for the tumor initiating activity of the EpCAM⁺/CAIX (high) population.

Discussion

Functional genomic screens using RNA interference have proven successful for the simultaneous identification and validation of novel genes involved in tumor progression. However, to date, no such study has been carried out with a clinically relevant primary tumor model for the identification of novel targets. Thus, a proof-of-concept study was carried out in patient-derived pancreatic tumor cells (PDX15). We simplified the size of the library and chose 12 genes, which were implicated in tumor metabolism and, consequently, in tumor growth. Thus, we found that shRNA hairpins for all 12 genes were differentially depleted in the final tumors. Although the genes chosen in the screen were reported in the literature to be strongly associated in tumorigenesis, we found great differences in representation (depletion frequency) of the 12 genes in the context of primary pancreatic tumor growth (PDX15). Thereafter, we focused on those targets that showed the highest and most consistent depletion of both the shRNA hairpins in the final tumors. Thus, 8 of the 12 shRNA pairs display less than <15% differences in percent inhibition of

tumor growth ($P < 0.05$). On a different note, we saw substantial variations in depletion frequencies of certain shRNA hairpins targeting the same gene (SGLT1, Glut1, ZIP4, and ASCT2; $P < 0.05$). Although, these shRNAs were prevalidated by *in vitro* knockdown assays, such results are not well understood. Plausible reasons for above results could be the altered stability and/or silencing efficiency of shRNA hairpins under *in vivo* environment. However, understanding the mechanisms of such outcome is beyond the scope of the current paper. In brief, our results demonstrate that PDX model could be a feasible tool for carrying out shRNA loss of function screen. Therefore, future shRNA screens could be carried out in PDX models derived from pancreatic and other indications.

xCT, a cysteine/glutamate antiporter that imports cysteine (the dimeric form of cysteine), is one of three amino acids required for glutathione synthesis. Detoxification of toxic compounds and amelioration of oxidative stress in tumor cells are critically dependent on this antioxidant. Due to this requirement, xCT is overexpressed in pancreatic and triple-negative breast cancer [28,29]. Previous reports indicate that forced reduction of xCT levels reduces viability of cancer

Table 1. Validation of Selected Genes *In Vivo* in the RAG2 KO Mouse Model

Summary of Individual shRNA knock down (KD) Data	
Treatment Arm	Tumor Take Rate
Untreated	6/6
Empty vector (pLKO)	6/8
CAIX-shRNA1	0/8
CAIX-shRNA2	0/8
MCT4-shRNA1	0/8
MCT4-shRNA2	0/8
xCT-shRNA1	0/8
xCT-shRNA2	0/8

Tumor take rate of the primary pancreatic tumor cells (PDX15) expressing shRNAs targeting CAIX (shRNA1 and shRNA2), xCT (shRNA1 and shRNA2), MCT4 (shRNA1 and shRNA2), empty vector (pLKO), and untreated control.

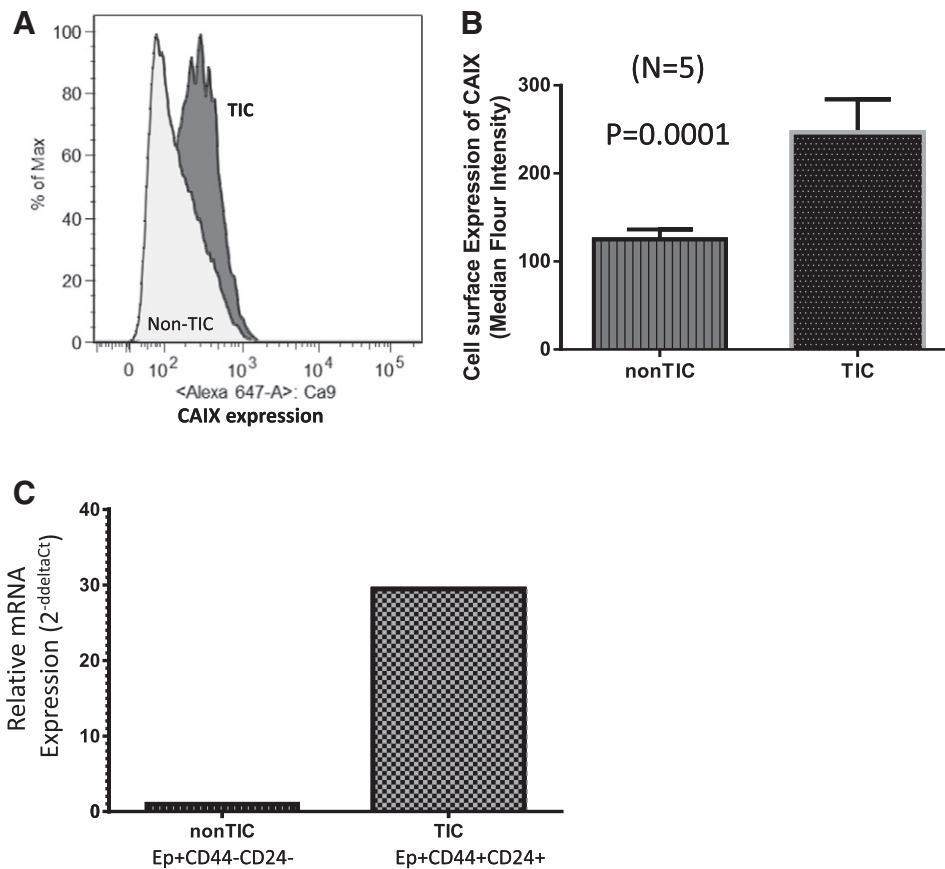


Figure 2. Increased expression of CAIX in primary pancreatic (PDX15) TICs versus non-TICs. (A) Assessment of CAIX cell surface levels in tumor initiating (EpCAM +/CD44 +/CD24 +) and non-tumor initiating (EpCAM +/CD44 -/CD24 -) populations. (B) Graphical representation of A. The graph describes median fluorescence of TIC and non-TIC populations. (C) Relative mRNA expression of TIC and non-TIC populations by TaqMan analysis.

cells either alone [20,21,30] or in combination with chemotherapeutics [29], and our results importantly extend these observations to a pancreatic PDX model. These results are significant because they suggest that some tumors are exclusively reliant on xCT to provide cysteine for glutathione synthesis and do not leverage other potentially redundant pathways as described earlier [31]. Increased reliance on xCT for import of cysteine for glutathione synthesis also suggests that targeting of this receptor will provide greater therapeutic margins than direct inhibition of glutathione synthesis that would be expected to result in wide-ranging toxicities [32]. Thus, xCT is considered an attractive target for cancer [28,29].

Activation of oncogenes reprogram cancer cells toward aerobic glycolysis to support their proliferation and growth, a phenomenon known as the Warburg effect [2]. Aerobic glycolysis is a fast route for production of ATP and other precursors required for synthesis of nucleotides, proteins, and lipids. Addiction of cancer cells to aerobic glycolysis therefore leads to accumulation of lactic acid. To maintain pH homeostasis, cells export lactic acid to prevent cellular acidification. MCT4 is one of four members of the solute carrier family 16A with symport H⁺ and lactate anions across the plasma membrane. Two of these members (MCT1 and MCT4) are mainly responsible for the efflux in cancer cells. As a result, elevated levels of MCT1 and MCT4 are characteristic of solid tumors and often associated with poor prognosis [33–36]. In particular, high MCT4 expression has been reported in renal, prostate, pancreatic, and

cervical cancers [34,37,38]. Several studies have further confirmed that silencing of MCT1 or MCT4 function significantly suppressed tumor growth in *in vivo* and *in vitro* models [7,38,39]. Thus, our data strongly corroborate these findings and suggest that MCT4 is required for primary pancreatic tumor (PDX15) growth.

CAIX was the top hit of the pooled shRNA screen. Hypoxia is a hallmark of many solid tumors, and CAIX is considered to be a marker for a hypoxic microenvironment. The regulation of CAIX by hypoxia-inducible transcription factor 1 and the role of CAIX in the regulation of pH dynamics in solid tumors are well characterized [22]. CAIX maintains pH homeostasis in cells and protects from the deleterious effects of acidosis caused by the high rate of aerobic glycolysis in tumors [22]. CAIX is an extracellular membrane-bound enzyme that catalyzes a hydration reaction that converts carbon dioxide to bicarbonate. Bicarbonate, in turn, is imported through specific transporters and promotes cell survival through buffering of intracellular pH [12]. In addition to its role in the regulation of tumoral pH and cell survival, there is evidence that suggests that CAIX is also involved in cell adhesion, migration, and metastasis [17]. Furthermore, silencing of CAIX expression in 4T1 mouse metastatic breast cancer cells resulted in regression of orthotopic mammary tumors and inhibition of spontaneous lung metastasis [18]. Likewise, stable depletion of CAIX in MDA-MB-231 human breast cancer xenografts also attenuated primary tumor growth [18]. Our results corroborate these findings and indicate that CAIX is an attractive target for cancer.

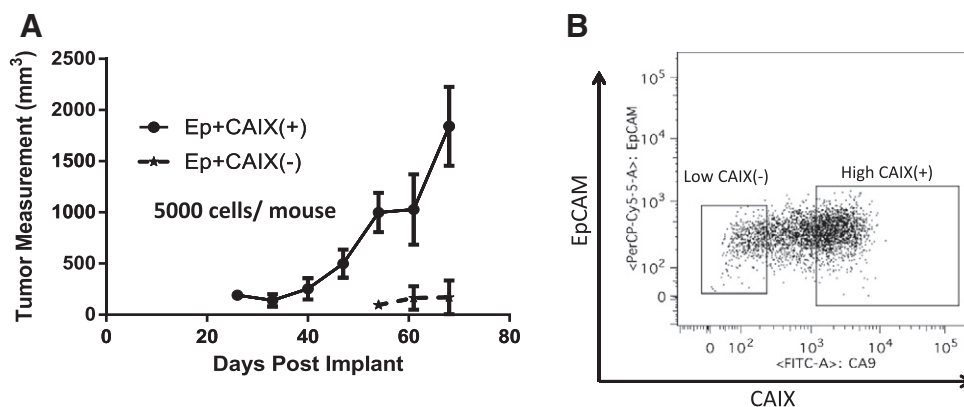


Figure 3. Increased tumor initiating potential of CAIX-enriched primary pancreatic tumor cells (PDX15). EpCAM+CAIX+ and EpCAM+CAIX- sorted cells from PDX15 tumors were implanted at indicated numbers in RAG2 KO mice. (A) Growth curve of EpCAM+CAIX+ and EpCAM+CAIX- phenotypes in RAG2 KO mice. Mice were implanted with 5000 cells of each population and were euthanized when tumor volume reached $\sim 2000 \text{ mm}^3$. (B) The gating strategy used to sort cells representing CAIX(+) or CAIX(-) phenotype.

Recent studies suggest that TICs have unique energy metabolism characteristics including low mitochondrial respiration and increased glycolysis for ATP generation [40]. TICs also prefer a hypoxic niche to maintain their “stemness” and tumor initiating potential [23,41,42]. These observations led us to evaluate expression of CAIX in the TIC and non-TIC populations of a pancreatic tumor model. CAIX is significantly overexpressed in TICs compared to non-TICs as confirmed by flow cytometry and qPCR analysis. Consistent with these observations, “stemness” markers, such as Oct4 and Nanog, and Epithelial mesenchymal transition (EMT) markers, like Snail and Twist, are also substantially overexpressed in CAIX-bearing TICs (data not shown). Additionally, our data demonstrate that CAIX-enriched epithelial cells (EpCAM+) of PDX15 display robust tumor initiation potential. As low as 100 cells (EpCAM+/CAIX+) were able to initiate palpable tumors in RAG2 KO mice. Recent data suggest that CAIX expression is required for the expression of EMT markers and may be involved in maintaining EMT status in breast cancer stem cells [23]. Our findings strongly corroborate the notion that cancer stem cells prefer a hypoxic niche to maintain their pluripotent potential and that CAIX plays an important role in survival in this metabolically altered, harsh microenvironment. Additionally, it is imperative to explore the abundance of CAIX expression in TICs of other solid tumors such as brain, colon, and head and neck, which often have a hypoxic microenvironment due to rapid cell division and aberrant blood vessel formation [43,44].

Genes identified as hits in an shRNA screen are predicted to be essential for autocrine growth pathways, while genes driving paracrine

growth are predicted to not be represented among the hits since the effects of their knockdown should be compensated for by the many neighboring cells knocked down in unrelated pathways and wild type for the paracrine pathway of interest. CAIX is predicted to be a paracrine actor since the bicarbonate produced by one cell should be available for import by neighboring cells. The fact that CAIX was detected in an autocrine pathway-focused shRNA screen suggests that it may have additional functions beyond CO_2 hydration. One plausible CO_2 -independent mechanism of action could be through p21 pathway regulation since this important cell cycle progression inhibitor has been shown to be upregulated following CAIX silencing [45]. Furthermore, it appears that loss of CAIX expression activates $\beta 1$ integrin pathways that may influence the proliferation of TICs. Thus, we hypothesize that the increased expression of CAIX may influence the survival and proliferation of TICs by the following two modalities: 1) by modulation of signaling pathways such as those involving p21 or $\beta 1$ integrin and 2) by regulation of extracellular pH (extrinsic factors), thus allowing TICs to thrive in a hypoxic and acidic microenvironment. Future experiments will compare the

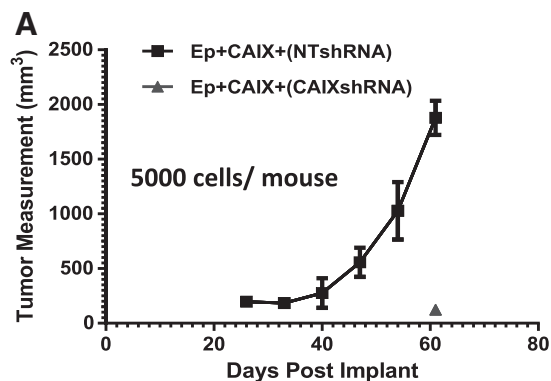


Figure 4. Silencing of CAIX expression by shRNAs significantly reduces tumor forming potential of PDX15. (A) Growth characteristics of CAIX-enriched EpCAM+ cells (5000 cells per mouse) that were transfected with either CAIX shRNAs (shRNA1 or shRNA2) or NT-shRNA.

Table 2. Summary of the Tumor Take Rate of EpCAM+/CAIX+ Cells

Cells Inoculated	Tumor Incidence		Comments
	CAIX(+)	CAIX(-)	
100	2(3)	1(3)	Ep+CAIX- tumors ~ 4 times smaller than Ep+CAIX+ tumors
500	7(8)	1(8)	Ep+CAIX- tumors ~ 4 times smaller than Ep+CAIX+ tumors
1000	6(10)	3(10)	Ep+CAIX- tumors ~ 6 times smaller than Ep+CAIX+ tumors
5000	4(4)	2(4)	Ep+CAIX- tumors ~ 8 times smaller than Ep+CAIX+ tumors

Take rate of CAIX+ and CAIX- populations in mice inoculated at the indicated cell numbers. For tumor incidence, the first number represents quantity of mice in which tumor grew, and the second number in parentheses represents the total number of mice inoculated.

Table 3. Tumors Take Rates of Transduced CAIX+ Populations. Number of Mice with Established Tumors 60 Days Following Inoculation with CAIX+ PDX15 Tumor Cells with or without CAIX Knockdown

Treatment Arm	Tumor Take Rate
NT-shRNA	5/5
CAIX-shRNA1	1/5
CAIX-shRNA2	0/5

ability of wild-type and catalytically inactive CAIX to rescue the effects of shRNA knockdown.

Since the introduction of the TIC concept, huge efforts have been invested to identify and characterize markers specific to TICs. As a consequence, overwhelming and steadily increasing numbers of such markers have been described [46,47]. To date, however, the function of such markers in TICs is still not fully understood. Our data suggest that CAIX is highly overexpressed in pancreatic TICs and could be used as a marker to identify and characterize these cells. Likewise, the expression of the other hits obtained from our shRNA screen could be further investigated to explore their requirement in TICs. Such efforts could identify novel markers or targets for TICs across various cancer types.

Overall, our data indicate that pooled shRNA screens in PDX models are a viable path for target discovery. We took an unbiased approach to successfully identify novel targets using bulk populations of PDX15. The design of the experiment was such that targets for both tumor initiation and tumor proliferation would be identified. Similar approaches could be exploited to identify novel targets from the TIC-enriched population but are beyond the scope of the current paper.

On the whole, our data indicate that inhibition of CAIX function may block both tumor initiation and proliferation. We propose that blocking of CAIX function with specific inhibitors and in combination with clinically approved or validated targeted therapies may lead to successful strategies to prevent tumor growth and metastasis in solid tumors.

Supplementary data to this article can be found online at <http://dx.doi.org/10.1016/j.neo.2015.05.001>.

Acknowledgements

We acknowledge Terry O'Day for his help in statistical analysis.

References

- Hanahan D and Weinberg RA (2011). Hallmarks of cancer: the next generation. *Cell* **144**, 646–674.
- Cairns RA, Harris IS, and Mak TW (2011). Regulation of cancer cell metabolism. *Nat Rev Cancer* **11**, 85–95.
- Elstrom RL, Bauer DE, Buzzai M, Karnauskas R, Harris MH, Plas DR, Zhuang H, Cinalli RM, Alavi A, and Rudin CM, et al (2004). Akt stimulates aerobic glycolysis in cancer cells. *Cancer Res* **64**, 3892–3899.
- Van Dyke T and Jacks T (2002). Cancer modeling in the modern era: progress and challenges. *Cell* **108**, 135–144.
- Zender L, Xue W, Zuber J, Semighini CP, Krasnitz A, Ma B, Zender P, Kubicka S, Luk JM, and Schirmacher P, et al (2008). An oncogenomics-based in vivo RNAi screen identifies tumor suppressors in liver cancer. *Cell* **135**, 852–864.
- Meacham CE, Ho EE, Dubrovsky E, Gertler FB, and Hemann MT (2009). In vivo RNAi screening identifies regulators of actin dynamics as key determinants of lymphoma progression. *Nat Genet* **41**, 1133–1137.
- Possemato R, Marks KM, Shaul YD, Pacold ME, Kim D, Birsoy K, Sethumadhavan S, Woo HK, Jang HG, and Jha AK, et al (2011). Functional genomics reveal that the serine synthesis pathway is essential in breast cancer. *Nature* **476**, 346–350.
- Miller PG, Al-Shahrour F, Hartwell KA, Chu LP, Jaras M, Puram RV, Puissant A, Callahan KP, Ashton J, and McConkey ME, et al (2013). In vivo RNAi screening identifies a leukemia-specific dependence on integrin beta 3 signaling. *Cancer Cell* **24**, 45–58.
- Daniel VC, Marchionni L, Hierman JS, Rhodes JT, Devereux WL, Rudin CM, Yung R, Parmigiani G, Dorsch M, and Peacock CD, et al (2009). A primary xenograft model of small-cell lung cancer reveals irreversible changes in gene expression imposed by culture in vitro. *Cancer Res* **69**, 3364–3373.
- Tentler JJ, Tan AC, Weekes CD, Jimeno A, Leong S, Pitts TM, Arcaroli JJ, Messersmith WA, and Eckhardt SG (2012). Patient-derived tumour xenografts as models for oncology drug development. *Nat Rev Clin Oncol* **9**, 338–350.
- Sorio C, Bonora A, Orlandini S, Moore P, Capelli P, Cristofori P, Dal Negro G, Marchiori P, Gaviraghi G, and Falconi M, et al (2001). Successful xenografting of cryopreserved primary pancreatic cancers. *Virchows Arch* **438**, 154–158.
- Chiche J, Ilc K, Laferriere J, Trotter E, Dayan F, Mazure NM, Brahimi-Horn MC, and Pouyssegur J (2009). Hypoxia-inducible carbonic anhydrase IX and XII promote tumor cell growth by counteracting acidosis through the regulation of the intracellular pH. *Cancer Res* **69**, 358–368.
- Ganapathy V, Thangaraju M, and Prasad PD (2009). Nutrient transporters in cancer: relevance to Warburg hypothesis and beyond. *Pharmacol Ther* **121**, 29–40.
- Izumi H, Torigoe T, Ishiguchi H, Uramoto H, Yoshida Y, Tanabe M, Ise T, Murakami T, Yoshida T, and Nomoto M, et al (2003). Cellular pH regulators: potentially promising molecular targets for cancer chemotherapy. *Cancer Treat Rev* **29**, 541–549.
- Fuchs BC and Bode BP (2005). Amino acid transporters ASCT2 and LAT1 in cancer: partners in crime? *Semin Cancer Biol* **15**, 254–266.
- Li M, Zhang Y, Liu Z, Bharadwaj U, Wang H, Wang X, Zhang S, Liuzzi JP, Chang SM, and Cousins RJ, et al (2007). Aberrant expression of zinc transporter ZIP4 (SLC39A4) significantly contributes to human pancreatic cancer pathogenesis and progression. *Proc Natl Acad Sci U S A* **104**, 18636–18641.
- Shin HJ, Rho SB, Jung DC, Han IO, Oh ES, and Kim JY (2011). Carbonic anhydrase IX (CA9) modulates tumor-associated cell migration and invasion. *J Cell Sci* **124**, 1077–1087.
- Lou Y, McDonald PC, Oloumi A, Chia S, Ostlund C, Ahmadi A, Kyle A, Auf dem Keller U, Leung S, and Huntsman D, et al (2011). Targeting tumor hypoxia: suppression of breast tumor growth and metastasis by novel carbonic anhydrase IX inhibitors. *Cancer Res* **71**, 3364–3376.
- Gerlinger M, Santos CR, Spencer-Dene B, Martinez P, Endesfelder D, Burrell RA, Vetter M, Jiang M, Saunders RE, and Kelly G, et al (2012). Genome-wide RNA interference analysis of renal carcinoma survival regulators identifies MCT4 as a Warburg effect metabolic target. *J Pathol* **227**, 146–156.
- Chung WJ, Lyons SA, Nelson GM, Hamza H, Gladson CL, Gillespie GY, and Sontheimer H (2005). Inhibition of cystine uptake disrupts the growth of primary brain tumors. *J Neurosci* **25**, 7101–7110.
- Savaskan NE, Heckel A, Hahnen E, Engelhorn T, Doerfler A, Ganslandt O, Nimsky C, Buchfelder M, and Eyupoglu IY (2008). Small interfering RNA-mediated xCT silencing in gliomas inhibits neurodegeneration and alleviates brain edema. *Nat Med* **14**, 629–632.
- McDonald PC, Winum JY, Supuran CT, and Dedhar S (2012). Recent developments in targeting carbonic anhydrase IX for cancer therapeutics. *Oncotarget* **3**, 84–97.
- Lock FE, McDonald PC, Lou Y, Serrano I, Chafe SC, Ostlund C, Aparicio S, Winum JY, Supuran CT, and Dedhar S (2013). Targeting carbonic anhydrase IX depletes breast cancer stem cells within the hypoxic niche. *Oncogene* **32**, 5210–5219.
- Li C, Heidt DG, Dalerba P, Burant CF, Zhang L, Adsay V, Wicha M, Clarke MF, and Simeone DM (2007). Identification of pancreatic cancer stem cells. *Cancer Res* **67**, 1030–1037.
- Hermann PC, Huber SL, Herrler T, Aicher A, Ellwart JW, Guba M, Bruns CJ, and Heeschen C (2007). Distinct populations of cancer stem cells determine tumor growth and metastatic activity in human pancreatic cancer. *Cell Stem Cell* **1**, 313–323.
- Herreros-Villanueva M, Zubia-Olascoaga A, and Bujanda L (2012). C-met in pancreatic cancer stem cells: therapeutic implications. *World J Gastroenterol* **18**, 5321–5323.
- Li C, Wu JJ, Hynes M, Dosch J, Sarkar B, Welling TH, Pasca di Magliano M, and Simeone DM (2011). C-met is a marker of pancreatic cancer stem cells and therapeutic target. *Gastroenterology* **141**, 2218–2227.e5.
- Lo M, Wang YZ, and Gout PW (2008). The x_c⁻ cystine/glutamate antiporter: a potential target for therapy of cancer and other diseases. *J Cell Physiol* **215**, 593–602.

- [29] Timmerman LA, Holton T, Yuneva M, Louie RJ, Padro M, Daemen A, Hu M, Chan DA, Ethier SP, and van 't Veer LJ, et al (2013). Glutamine sensitivity analysis identifies the xCT antiporter as a common triple-negative breast tumor therapeutic target. *Cancer Cell* **24**, 450–465.
- [30] Gout PW, Buckley AR, Simms CR, and Bruchovsky N (2001). Sulfasalazine, a potent suppressor of lymphoma growth by inhibition of the x_c⁻ cystine transporter: a new action for an old drug. *Leukemia* **15**, 1633–1640.
- [31] Danbolt NC (2001). Glutamate uptake. *Prog Neurobiol* **65**, 1–105.
- [32] Estrela JM, Ortega A, and Obrador E (2006). Glutathione in cancer biology and therapy. *Crit Rev Clin Lab Sci* **43**, 143–181.
- [33] Miranda-Goncalves V, Honavar M, Pinheiro C, Martinho O, Pires MM, Pinheiro C, Cordeiro M, Bebiano G, Costa P, and Palmeirim I, et al (2013). Monocarboxylate transporters (MCTs) in gliomas: expression and exploitation as therapeutic targets. *Neuro Oncol* **15**, 172–188.
- [34] Pinheiro C, Longatto-Filho A, Scapulatempo C, Ferreira L, Martins S, Pellerin L, Rodrigues M, Alves VA, Schmitt F, and Baltazar F (2008). Increased expression of monocarboxylate transporters 1, 2, and 4 in colorectal carcinomas. *Virchows Arch* **452**, 139–146.
- [35] Pinheiro C, Albergaria A, Paredes J, Sousa B, Dufloth R, Vieira D, Schmitt F, and Baltazar F (2010). Monocarboxylate transporter 1 is up-regulated in basal-like breast carcinoma. *Histopathology* **56**, 860–867.
- [36] de Oliveira AT, Pinheiro C, Longatto-Filho A, Brito MJ, Martinho O, Matos D, Carvalho AL, Vazquez VL, Silva TB, and Scapulatempo C, et al (2012). Co-expression of monocarboxylate transporter 1 (MCT1) and its chaperone (CD147) is associated with low survival in patients with gastrointestinal stromal tumors (GISTs). *J Bioenerg Biomembr* **44**, 171–178.
- [37] Pertega-Gomes N, Vizcaino JR, Miranda-Goncalves V, Pinheiro C, Silva J, Pereira H, Monteiro P, Henrique RM, Reis RM, and Lopes C, et al (2011). Monocarboxylate transporter 4 (MCT4) and CD147 overexpression is associated with poor prognosis in prostate cancer. *BMC Cancer* **11**, 312 [2407-11-312].
- [38] Zhu J, Wu YN, Zhang W, Zhang XM, Ding X, Li HQ, Geng M, Xie ZQ, and Wu HM (2014). Monocarboxylate transporter 4 facilitates cell proliferation and migration and is associated with poor prognosis in oral squamous cell carcinoma patients. *PLoS One* **9**, e87904.
- [39] Le Floch R, Chiche J, Marchiq I, Naiken T, Ilc K, Murray CM, Critchlow SE, Roux D, Simon MP, and Pouyssegur J (2011). CD147 subunit of lactate/H⁺ symporters MCT1 and hypoxia-inducible MCT4 is critical for energetics and growth of glycolytic tumors. *Proc Natl Acad Sci U S A* **108**, 16663–16668.
- [40] Zhou Y, Zhou Y, Shingu T, Feng L, Chen Z, Ogasawara M, Keating MJ, Kondo S, and Huang P (2011). Metabolic alterations in highly tumorigenic glioblastoma cells: preference for hypoxia and high dependency on glycolysis. *J Biol Chem* **286**, 32843–32853.
- [41] Keith B and Simon MC (2007). Hypoxia-inducible factors, stem cells, and cancer. *Cell* **129**, 465–472.
- [42] Heddleston JM, Li Z, Lathia JD, Bao S, Hjelmeland AB, and Rich JN (2010). Hypoxia inducible factors in cancer stem cells. *Br J Cancer* **102**, 789–795.
- [43] Carmeliet P and Jain RK (2000). Angiogenesis in cancer and other diseases. *Nature* **407**, 249–257.
- [44] Pouyssegur J, Dayan F, and Mazure NM (2006). Hypoxia signalling in cancer and approaches to enforce tumour regression. *Nature* **441**, 437–443.
- [45] Doyen J, Parks SK, Marcie S, Pouyssegur J, and Chiche J (2013). Knock-down of hypoxia-induced carbonic anhydrases IX and XII radiosensitizes tumor cells by increasing intracellular acidosis. *Front Oncol* **2**, 199.
- [46] Karsten U and Goletz S (2013). What makes cancer stem cell markers different? *Springerplus* **2**, 301.
- [47] Keysar SB and Jimeno A (2010). More than markers: biological significance of cancer stem cell-defining molecules. *Mol Cancer Ther* **9**, 2450–2457.